*J. Fluid Mech.* (2022), *vol*. 948, A55, doi:10.1017/jfm.2022.734

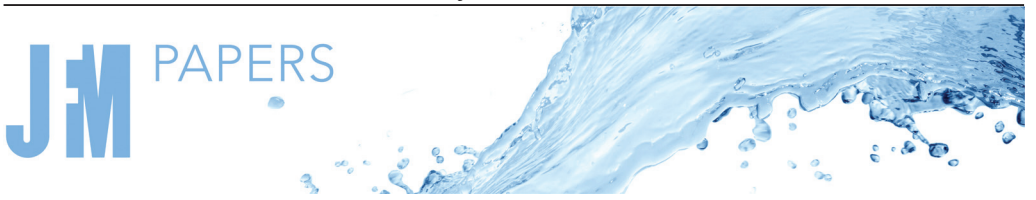

# Inertio-thermal vapour bubble growth

**Patrick Sullivan[1],†, Duncan Dockar[1], Matthew K. Borg[1], Ryan Enright[2] and Rohit Pillai[1]**

[1]Institute for Multiscale Thermofluids, University of Edinburgh, Edinburgh EH9 3FB, UK

[2]Thermal Management Research, *η*et department, Nokia Bell Labs, 600 Mountain Av., Murray Hill, NJ 07974, USA

(Received 9 February 2022; revised 15 August 2022; accepted 21 August 2022)

Our understanding of homogeneous vapour bubble growth is currently restricted to asymptotic descriptions of their limiting behaviour. While attempts have been made to incorporate both the inertial and thermal limits into bubble growth models, the early stages of bubble growth have not been captured. By accounting for both the changing inertial driving force and the thermal restriction to growth, we present an inertio-thermal model of homogeneous vapour bubble growth, capable of accurately capturing the evolution of a bubble from the nano- to the macro-scale. We compare our model predictions with: (*a*) published experimental and numerical data, and (*b*) our own molecular simulations, showing significant improvement over previous models. This has potential application in improving the performance of engineering devices, such as ultrasonic cleaning and microprocessor cooling, as well as in understanding of natural phenomena involving vapour bubble growth.

**Key words:** bubble dynamics, condensation/evaporation

## 1. Introduction

Vapour bubble growth has long been an area of scientific interest, as they underpin numerous natural phenomena (Prosperetti 2017) and engineering applications, such as ultrasonic cleaning (Yasui 2018) and two-phase thermal management systems (Robinson & Judd 2004). Vapour bubble growth can also have deleterious effects; for example, they have been shown to play a significant role in the explosive failure of pressurised containers (Reinke 1997) and the dryout failure of pool boiling systems (Chu *et al.* 2013).

† Email address for correspondence: patrick.sullivan@ed.ac.uk

Understanding the growth behaviour of vapour bubbles is therefore an important open problem, and current theoretical models remain incomplete.

In one of the earliest theoretical analyses on homogeneous vapour bubble growth, Plesset & Zwick (1954) equated the latent heat required to grow the bubble to the heat available through conduction. Their Plesset–Zwick (PZ) model predictions showed excellent agreement with experimental results for water (Dergarabedian 1953) and later for other fluids (Dergarabedian 1960; Florschuetz, Henry & Khan 1969). However, the PZ model was subsequently shown to significantly overpredict the growth of bubbles at reduced pressures (Lien 1969), where there is an increased time scale at which thermal effects dominate the bubble's growth. This overprediction results from an unphysical infinite initial velocity, instead of being limited by inertial forces until the thermal time scale has been reached.

Mikic, Rohsenow & Griffith (1970) accounted for this inertial limit and derived a formula that interpolates between the inertial velocity given by Rayleigh (1917) and the thermal velocity of Plesset & Zwick (1954); their model is now commonly referred to as the Mikic–Rohsenow–Griffith (MRG) model. The MRG model removes the infinite initial velocity predicted by the PZ model, instead bounding it by the inertial limit, which then better matched experimental data (Lien 1969). While the MRG model accurately captures the transition between the inertial- and thermal-limiting velocities, it still overpredicts the growth of an initially static bubble, as it assumes a finite initial velocity. Additionally, there does not exist a model capable of capturing the effects of capillarity and viscosity, which are both relevant to early-stage growth (Avdeev 2016).

This theoretical bottleneck, coupled with the difficulties in obtaining high-resolution data for isolated bubble growth, has led to the development of numerical techniques for the measurement of bubble growth rates (Dalle Donne & Ferranti 1975; Lee & Merte 1996). These numerical investigations have been used to show excellent agreement with the existing theories, failing only when the assumptions made by the theories are shown to be invalid (Robinson & Judd 2004). Most numerical models solve the coupled momentum and energy differential equations, with varying approximations for the treatment of heat transfer in the thermal boundary layer (Prosperetti & Plesset 1978). Recent works have investigated the approximations typically made in the momentum equation, such as Bardia & Trujillo (2019), who added the effects of mass transfer across the bubble interface. While these numerical studies provide high-resolution data for the growth of vapour bubbles, they do not provide additional clarity to the understanding of the relationship between the inertial and thermal limitations on bubble growth rates that can be obtained from an analytical model.

In this paper we present a new class of inertio-thermal models for the growth of vapour bubbles that captures the competition between inertial and thermal effects on bubble growth. We find that the entire lifetime of the bubble can be modelled by limiting the growth by the available inertia. When compared with existing experimental and numerical data, we show better agreement than the MRG model. We are able to incorporate viscous and capillary effects that are required for nanoscale bubble growth, with comparisons against our own molecular simulations.

## 2. Model formulation

### 2.1. *Inertial bubble growth*

In the absence of thermal effects, the growth of a spherical vapour bubble with vapour pressure $P_v$ surrounded by a liquid at pressure $P_\infty$ is described by the generalised

Rayleigh–Plesset (RP) equation for Newtonian fluids (Prosperetti 1982)

$$R\dot{U}_l + \frac{3}{2}U_l^2 - \frac{J}{\rho_l}\left[2U_l + J\left(\frac{1}{\rho_v} - \frac{1}{\rho_l}\right)\right] = \frac{1}{\rho_l}\left(P_v - P_\infty - \frac{2\gamma}{R} - \frac{4\mu U_l}{R}\right), \tag{2.1}$$

where $R$ and $U_l$ represent the bubble radius and the radial velocity in the liquid at the interface, respectively, with dots used to represent their time derivatives; while $\rho_l$, $\gamma$ and $\mu$ represent the liquid's density, surface tension and dynamic viscosity, respectively. The term $\rho_v$ represents the density of the vapour and $J$ is the mass flux across the liquid–vapour interface. The mass flux can be used to relate the radial velocity of the bubble $\dot{R}$ to the velocity of the liquid at the interface $J = \rho_l(U_l - \dot{R})$. For cases away from the critical point, where $\rho_l \gg \rho_v$, the contribution of mass transfer can be neglected, giving the classical RP equation (details in supplementary material available at https://doi.org/10.1017/jfm.2022.734)

$$R\ddot{R} + \frac{3}{2}\dot{R}^2 = \frac{1}{\rho_l}\left(P_v - P_\infty - \frac{2\gamma}{R} - \frac{4\mu\dot{R}}{R}\right). \tag{2.2}$$

We can see from (2.2) that the stationary case of this model, i.e. when $\dot{R} = \ddot{R} = 0$, returns the critical radius from nucleation theory $R_c = 2\gamma/\Delta P$ (Kaschiev 2000, p. 49), where $\Delta P$ is the difference between liquid and vapour pressure, i.e. $\Delta P = P_v - P_\infty$. By integrating (2.2), it has been shown that the inertial bubble velocity reaches a maximum value of $A$, given as (Prosperetti 2017)

$$\dot{R}_{RP,max} = A = \sqrt{\frac{2\Delta P}{3\rho_l}}. \tag{2.3}$$

Taking the initial acceleration of $\ddot{R} = \Delta P/\rho_l R_0$ (Brennen 2013, p. 38), the time taken by a stationary bubble of initial size $R_0$ to reach this inertial velocity $A$, can be approximated as

$$\tau_{RP} = \frac{A}{\ddot{R}} = R_0\sqrt{\frac{2\rho_l}{3\Delta P}}. \tag{2.4}$$

### 2.2. *Thermal bubble growth*

Inertial bubble growth continues as long as the pressure difference across the bubble interface is maintained. However, in reality, heat must be conducted through the liquid as the bubble grows in order to balance the latent heat of vaporisation required to grow the bubble. This results in a drop in the bubble vapour pressure $P_v$ as it grows, and therefore a drop in the pressure difference $\Delta P$. In this section, an overview of existing thermally limited bubble growth models is provided.

Plesset & Zwick (1954) assumed that this heat is conducted through a thin thermal boundary layer, and equated it to the latent heat to obtain an expression for bubble velocity during thermally limited growth (details in the supplementary material)

$$\dot{R}_{PZ} = Ja\sqrt{\frac{3\alpha}{\pi t}}, \tag{2.5}$$

where $\alpha = k/\rho_l c_p$ is the thermal diffusivity of the liquid, $k$ is the thermal conductivity and $c_p$ is the specific heat capacity. The Jakob number $Ja$, is the ratio of sensible heat to latent

heat, given by $Ja = \rho_l c_p \Delta T_0 / \rho_v h_{lv}$, where $\Delta T_0$ is the initial liquid superheat, and $h_{lv}$ is the enthalpy of vaporisation.

Mikic *et al.* (1970) rewrote (2.5) in the form

$$\dot{R}_{PZ} = \frac{B}{2\sqrt{t}}\left(1 - \frac{T_v - T_{sat}}{\Delta T_0}\right), \tag{2.6}$$

where $B = Ja\sqrt{12\alpha/\pi}$, $T_v$ is the instantaneous vapour temperature and $T_{sat}$ is the saturation temperature of the liquid. Assuming that the instantaneous superheat and pressure difference vary linearly (Theofanous & Patel 1976; Lee & Merte 1996) i.e.

$$\frac{T_v - T_{sat}}{\Delta T_0} = \frac{P_v - P_\infty}{\Delta P_0}, \tag{2.7}$$

where $\Delta P_0$ is the initial pressure difference, (2.5) can now be rewritten in terms of the instantaneous pressure difference, $P_v - P_\infty$

$$P_v - P_\infty = \Delta P_0\left(1 - \frac{2\sqrt{t}}{B}\dot{R}\right), \tag{2.8}$$

where we have used $\dot{R}$ in place of $\dot{R}_{PZ}$ to clarify that the pressure difference varies with bubble velocity, consistent with literature on this topic (Prosperetti 1982; Lee & Merte 1996).

Mikic *et al.* (1970) then modified the inertial-limiting velocity (2.3) presented in the previous section by using the instantaneous (time-varying) pressure difference to recalculate the velocity rather than the initial (constant) pressure difference typically used, resulting in the MRG model. Thus, the MRG model accounts for the change in vapour pressure as the bubble grows and cools, producing a quadratic equation for $\dot{R}$. This is expressed in terms of the initial limiting velocity $A_0$, calculated using the initial pressure difference $\Delta P_0$. The negative root of this equation was rejected, giving

$$\dot{R}_{MRG} = A_0\left[\sqrt{\frac{A_0^2}{B^2}t + 1} - \sqrt{\frac{A_0^2}{B^2}t}\right]. \tag{2.9}$$

Equation (2.9) represents an improvement over the PZ model (2.5) as it extends the applicability of the model to earlier stages of bubble growth, removing the non-physical infinite initial velocity that would be obtained if the PZ model were extrapolated (as $t \to 0$, $\dot{R}_{PZ} \to \infty$ while $\dot{R}_{MRG} \to A$). The MRG model has been shown to accurately predict the transition from inertially limited to thermally limited bubble growth (Lee & Merte 1996; Robinson & Judd 2004). Importantly, it sets the time scale

$$\tau_{MRG} = \frac{B^2}{A^2}, \tag{2.10}$$

when thermal effects cause the bubble growth to diverge from the inertial limit. Several papers have since made modifications to this model to better capture vapour bubble growth (Board & Duffey 1971; Theofanous & Patel 1976; Prosperetti & Plesset 1978). These modifications generally involve using a different relationship between the vapour pressure and temperature difference, typically a direct linear relationship (Lee & Merte 1996; Robinson & Judd 2004), instead of the Clausius–Clapeyron approximation originally used by Mikic *et al.* (1970).

While the MRG model is an improvement over the PZ model, it still assumes that the bubble begins growing at the inertial-limiting velocity $A$, ignoring the finite time required for the bubble to reach this velocity from rest. This assumption implies an infinite radial acceleration in the case of an initially static bubble, which is clearly non-physical. In this work, we account for the finite acceleration of initially static vapour bubbles rather than assuming the limiting value from (2.3), as elaborated in the next section.

### 2.3. *Inertio-thermal bubble growth*

While (2.2) is challenging to solve analytically in its full form, an analytical solution can be obtained for the inviscid case ($\mu = 0$) (Dergarabedian 1953). However, this solution only provides the time taken for bubble growth for a given radius, and cannot be inverted to obtain an equation for the temporal variation in bubble radius. This prevents us from using a fully analytical solution to the RP equation with a time-varying vapour pressure, even in the case of zero viscosity.

Instead, we develop a simplified model for the radial velocity in the absence of capillary and viscous effects ($\mu = \gamma = 0$) following the methodology of Avdeev (2016, pp. 55–58). The RP equation (2.2) can be written in the simplified form (Brennen 2013, p. 37)

$$\dot{R}_{RP} = A\sqrt{1 - \left(\frac{R_0}{R}\right)^3}. \tag{2.11}$$

Avdeev then integrates this expression in the limits of $R \to R_0$ and $R \to \infty$ and provides a simpler approximation for the radius

$$R = \frac{R_0}{3} + \frac{2R_0}{3}\sqrt{1 + \frac{t^2}{\tau_{RP,0}^2}}, \tag{2.12}$$

by assuming a constant pressure difference $\Delta P_0$, with $\tau_{RP,0}$ representing the corresponding inertial time scale from (2.4), computed using $\Delta P_0$ instead of $\Delta P$. Taking the time derivative of (2.12) returns the following approximation for the original expression given in (2.11):

$$\dot{R}_{RP,0} = \frac{A_0}{\sqrt{1 + \dfrac{\tau_{RP,0}^2}{t^2}}}. \tag{2.13}$$

This model interpolates between the linearly increasing velocity expected in the initial stages of the bubble growth ($\dot{R} \approx \ddot{R}t$) and the constant velocity in the late stages, when the velocity has reached the inertial limit ($\dot{R} \approx A_0$). This model has been shown to give excellent agreement with the exact solution (Avdeev 2016, p. 58).

#### 2.3.1. *Full inertio-thermal model*

Using this simple model for the evolution of the bubble's radius, we can now develop a new model for the instantaneous velocity of the bubble $\dot{R}_{RP,i}$, accounting for the change in pressure as the bubble grows. As Avdeev (2016, pp. 55–58) did for constant pressure, we interpolate between the early and late stages of growth. In the early stages of growth, for $t \ll \tau_{RP}$, the radial velocity is given as $\dot{R} = \ddot{R}t = At/\tau_{RP}$. Similarly, in the late stages

of growth, for $t \gg \tau_{RP}$, the radial velocity is given by $\dot{R} = A$. Interpolating between these values gives us

$$\dot{R}_{RP,i} = \frac{A}{\sqrt{1 + \dfrac{\tau_{RP}^2}{t^2}}}, \tag{2.14}$$

which describes the acceleration of the bubble from rest to its limiting value $A$, with a time scale of $\tau_{RP}$ (as opposed to $A_0$ and $\tau_{RP,0}$, respectively, in (2.13)). Note it is the term in the denominator that ensures the bubble velocity starts from zero, which is missing from (2.3) and therefore the MRG model (2.9). Equation (2.14) is equivalent to allowing the pressure to change over time in the velocity expression calculated from (2.13).

Following Mikic *et al.* (1970), we substitute the instantaneous pressure difference from (2.8) into our new inertial growth equation (2.14), and treat the radial velocity terms as equivalent. We then obtain the following expression:

$$\dot{R} = \sqrt{\frac{A_0^2}{1 + \dfrac{\tau_{RP,0}^2}{t^2\left(1 - \dfrac{2\sqrt{t}}{B}\dot{R}\right)}}\left(1 - \frac{2\sqrt{t}}{B}\dot{R}\right)}, \tag{2.15}$$

where $A_0^2(1 - (2\sqrt{t}/B)\dot{R}) = A^2$ and $\tau_{RP,0}^2/(1 - (2\sqrt{t}/B)\dot{R}) = \tau_{RP}^2$, from (2.3) and (2.4), respectively. Here, we switch from $\dot{R}_{RP}$ to $\dot{R}$ to equate the radial velocity terms, as was done with the MRG model. This expression accounts for the thermal effects on both the inertial-limiting velocity $A$ and on the inertial time scale $\tau_{RP}$. Rearranging (2.15) gives a cubic expression in $\dot{R}$

$$\frac{2\sqrt{t}}{B}\dot{R}^3 + \left(\frac{4A_0^2 t}{B^2} - 1 - \frac{\tau_{RP,0}^2}{t^2}\right)\dot{R}^2 - \frac{4A_0^2\sqrt{t}}{B}\dot{R} + A_0^2 = 0, \tag{2.16}$$

which can be solved analytically using Cardano's formula. The solution to equation (2.16) is what we refer to as the full inertio-thermal (FIT) model. While it can be shown that the three roots to equation (2.16) are real through discriminant analysis, the roots can only be expressed in a complex form (details in the supplementary material). For the case of $\tau_{RP,0} = 0$, corresponding to the velocity initially having a value equal to the inertial limit, the roots of the equation are exactly the PZ model (2.5), the rejected negative result from the MRG derivation and the MRG model (2.9), respectively. As the FIT model presents as a complex equation, we can alternatively find approximations to the solutions of (2.16), which are less accurate than the FIT, but potentially more useful. These approximations further allow us to include the effects of capillarity and viscosity, which are not accounted for in (2.14).

### 2.3.2. *Approximate inertio-thermal model*

If we return to the derivation of (2.13), the assumption of constant pressure difference manifests in the integral (Avdeev 2016, p. 55)

$$\int_0^t \frac{A}{R_0}\mathrm{d}t \approx \frac{3t}{2\tau_{RP,0}}. \tag{2.17}$$

If we substitute the integral from (2.17) into (2.12) rather than the approximated value, we retrieve an expression for the radius of the bubble with a time-varying pressure

$$R = \frac{R_0}{3} + \frac{2R_0}{3}\sqrt{1 + \left(\frac{3\displaystyle\int_0^t \frac{A}{R_0}\mathrm{d}t}{2}\right)^2}. \tag{2.18}$$

Taking the time derivative of (2.18) gives us an approximation for the radial velocity with varying pressure

$$\dot{R}_{RP,i} = \frac{A}{\sqrt{1 + \left(\dfrac{2}{3\displaystyle\int_0^t \frac{A}{R_0}\mathrm{d}t}\right)^2}}. \tag{2.19}$$

Taking $A = A_0\sqrt{1 - (2\sqrt{t}/B)\dot{R}}$ as before, the integral term in (2.19) can be approximated by taking a Taylor series expansion around $t = 0$ giving

$$\int_0^t \frac{A}{R_0}\mathrm{d}t = \frac{A_0}{R_0}\int_0^t \sqrt{1 - \frac{2\sqrt{t}}{B}\dot{R}}\,\mathrm{d}t = \frac{A_0}{R_0}\left(t - \frac{2t^{3/2}\dot{R}(0)}{3B} - \frac{t^2\dot{R}(0)^2}{4B^2} + O(t^{5/2})\right). \tag{2.20}$$

Evaluating this approximation for the initially static case $\dot{R}(0) = 0$ and ignoring the higher-order terms lets us approximate equation (2.19) as

$$\dot{R} = \frac{A_0\sqrt{1 - \dfrac{2\sqrt{t}}{B}\dot{R}}}{\sqrt{1 + \dfrac{\tau_{RP,0}^2}{t^2}}}. \tag{2.21}$$

Solving this expression for $\dot{R}$ gives

$$\dot{R}_{AIT} = \frac{A_0}{\sqrt{1 + \dfrac{\tau_{RP,0}^2}{t^2}}}\left[\sqrt{\frac{A_0^2}{B^2\left(1 + \dfrac{\tau_{RP,0}^2}{t^2}\right)}t + 1} - \sqrt{\frac{A_0^2}{B^2\left(1 + \dfrac{\tau_{RP,0}^2}{t^2}\right)}t}\right], \tag{2.22}$$

which we will refer to as the approximate inertio-thermal (AIT) model. Alternatively, rather than the above process, we can directly replace the inertial-limiting velocity $A_0$ in the MRG model (2.9) with the instantaneous velocity from (2.14), which again gives (2.22).

The AIT accounts for the need for the bubble to have grown (and phase change to have occurred), in order for the temperature gradient to form in the liquid. We can rewrite the

AIT model more generally in terms of the instantaneous velocity predicted by the constant pressure RP model equation (2.13), $\dot{R}_{RP,0}$, as

$$\dot{R}_{AIT} = \dot{R}_{RP,0}\left[\sqrt{\frac{\dot{R}_{RP,0}^2}{B^2}t + 1} - \sqrt{\frac{\dot{R}_{RP,0}^2}{B^2}t}\right]. \tag{2.23}$$

This allows us to include the effects of capillarity and viscosity in our model through the calculation of the inertial velocity $\dot{R}_{RP,0}$ directly from (2.2). This is achieved in our case by numerically calculating the value using a Runge–Kutta ordinary differential equation (ODE) solver.

The AIT model offers us a clearer insight into the coupling of inertial and thermal effects in the growth of vapour bubbles. We can now see how the inertial growth of the bubble causes the heat transfer behaviour to change. As the bubble accelerates, a greater heat transfer rate is required to maintain the growth, slowing down the bubble's velocity. Similarly, the model captures how, in the absence of significant inertial effects, the time scale for thermal diffusion controlled growth can be significantly increased. Most importantly, the effects of surface tension and viscosity can be included in the AIT model by explicitly calculating the value of $\dot{R}_{RP,0}$ from (2.2) (note that this is not possible in the FIT model). Using this model we can now better understand the coupled inertia and thermal diffusion effects on the growth of vapour bubbles when capillarity and viscosity are relevant.

### 2.3.3. *Simple inertio-thermal model*

In cases when the ratio of the inertial time scale $\tau_{RP}$ (2.4) to the thermal time scale $\tau_{MRG}$ (2.10) is low i.e. for $\tau_{RP}/\tau_{MRG} < 1$, inertial effects occur on a faster time scale than thermal effects, allowing them to be treated as independently changing parameters. This allows further simplification of the AIT model as the bubble will have approached its inertial-limiting velocity before thermal effects on growth are significant, giving

$$\dot{R}_{SIT} = \frac{\dot{R}_{RP,0}\dot{R}_{MRG}}{A_0}. \tag{2.24}$$

We call (2.24) the simple inertio-thermal (SIT) model. As with the AIT model, when $t \gg \tau_{RP,0}$ the effect of changing inertia can be disregarded in the SIT model as well. In addition, when $t \ll \tau_{MRG}$, the $\tau_{RP,0}/t$ terms in (2.22) can be disregarded, justifying the simplification in (2.24). Again, capillary and viscous effects can be included by explicitly calculating the instantaneous inertial velocity term $\dot{R}_{RP,0}$ from (2.2). In general, we can perform this simplification and use the SIT model whenever $\tau_{RP} < \tau_{MRG}$.

The FIT, AIT and SIT models, from (2.16), (2.22) and (2.24), respectively, represent a new class of inertio-thermal models for vapour bubble growth. For the cases with $\tau_{RP} < \tau_{MRG}$, the SIT model can be used, as inertial and thermal effects occur on different time scales. For $\tau_{RP} > \tau_{MRG}$, the AIT model should be used, as it captures the interaction between inertial and thermal effects. The FIT can be used for all time scale ratios, but only in the absence of viscous and capillary effects. An analysis of the agreement of the three models has been presented in the SI, highlighting the poor agreement of the SIT model for $\tau_{RP} > \tau_{MRG}$, but an improved agreement for $\tau_{RP} < \tau_{MRG}$.

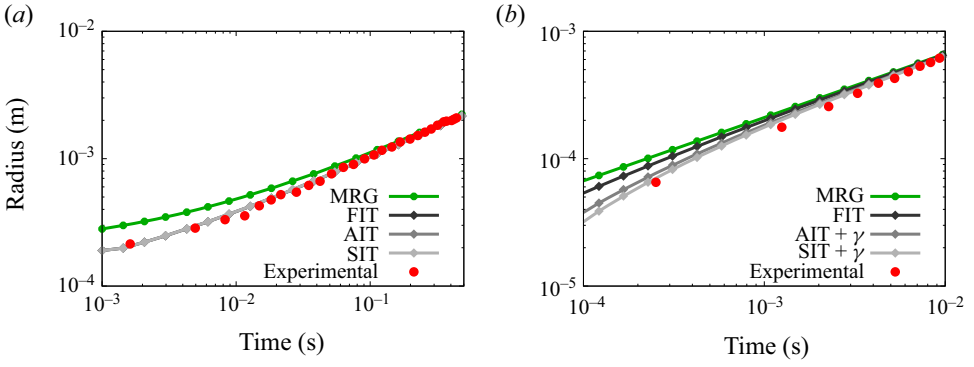


Figure 1. Comparisons of the predictions of the MRG and our IT models with the experimental work of (*a*) Florschuetz *et al.* (1969), and (*b*) Dergarabedian (1953). Note the symbol $\gamma$ in (*b*) represents the inclusion of surface tension in the calculation of the AIT and SIT models.

## 3. Model validation

### 3.1. *In the absence of viscous and capillary effects*

We can quantify the effect of capillarity through the ratio of the bubble's initial radius to the critical radius $\mathcal{R} = R_0/R_c$. The effect of viscosity can be quantified by the Reynolds number, $Re = A_0 R_0 \rho_l/\mu$. We would expect the capillary and viscous effects to be greater for lower values of $\mathcal{R}$ and $Re$, respectively. In the absence of viscous and capillary effects, we would expect our inertio-thermal model to deviate most from the MRG model predictions when the thermal time scale is smaller than the inertial, i.e. $\tau_{RP}/\tau_{MRG} > 1$. The experiments of Florschuetz *et al.* (1969) meet this criterion as $\tau_{RP}/\tau_{MRG} \approx 42.5 > 1$. The effects of capillarity and viscosity can be neglected for this case as $\mathcal{R} \approx 60$ and $Re \approx 1700$.

The predictions of the MRG (2.9) and inertio-thermal (IT) models are compared with the data in Florschuetz *et al.* (1969) in figure 1(*a*). We can see from the figure that the IT models better describe the early stages of the bubble's growth. The initial inertial velocity predicted by the MRG model overpredicts the actual growth rate. In the latter stages of the bubble's growth, the velocities predicted by both models converge to the limiting value of the PZ model. Therefore, in the absence of viscous and capillary effects, the MRG model overpredicts the experimental data overall, while the IT model predictions (which lie on top of each other) are more accurate. In this case, we see good agreement between all three IT models, as there are no effects of capillarity or viscosity.

It is worth noting that the results reported by Florschuetz *et al.* (1969) were for reasonably isolated bubbles that nucleated in the bulk liquid. This ensured that the thermal boundary layer of the bubble was not disrupted by the presence of other bubbles or the walls of the test vessel during the measurement period. In contrast to Lien (1969), where the maximum disruption to the thermal boundary layer was expected in the early stages of growth due to the electrodes used caused the bubble nucleation, Florschuetz *et al.* (1969) nucleated bubbles on natural nucleation sites in the bulk liquid. In this case, the greatest deviation from theory is expected in the later stages of growth, when the bubble has grown sufficiently large for its thermal boundary layer to interact with the surroundings. For this reason, we can attribute the disagreement of the early stage experimental results and the MRG model to the limiting inertia and not the presence of other bubbles or walls.

### 3.2. *The effect of capillarity*

Capillary effects become important in determining the growth of bubbles when they are close to the critical size. In these cases, the available hydrodynamic pressure in the bubble is reduced by the Laplace pressure across the interface. Both numerical (Lee & Merte 1996; Robinson & Judd 2004) and experimental (Dergarabedian 1960) studies have focused on the growth of critically sized bubbles. One of the earliest such studies was that of Dergarabedian (1953), who experimentally measured the growth of vapour bubbles at low superheats. The case shown in figure 1(*b*) is of the growth of a water vapour bubble at a superheat of $\Delta T = 3.1$ K. The bubble is grown from close to the critical radius, with $\mathcal{R} \approx 1.05$. The effect of viscosity can be neglected as $Re \approx 100$. The SIT model (with capillary effects included, shown as SIT $+ \gamma$ in figure 1*b*) can be used to predict the bubble growth here, as $\tau_{RP} < \tau_{MRG}$ ($\tau_{RP} \approx 2.3$ µs and $\tau_{MRG} \approx 5.3$ µs). The SIT model allows us to use the exact inertial velocity, calculated from numerically integrating the RP equation (2.2), which includes the effects of capillarity, using a Runge–Kutta ODE solver. We can see from figure 1(*b*) that the SIT curve provides better agreement with the experimental data than the MRG model, most notably during the earlier stages of growth. The AIT model (with capillary effects included, shown as AIT $+ \gamma$ in figure 1*b*) also provides good agreement for the growth of the bubble, predicting a slightly higher radius than the SIT model. The FIT model, which does not include capillary effects, does not show the same level of agreement. In this case, when capillarity dominates the early stage growth behaviour, the FIT model predicts bubble radii noticeably closer to those of the MRG model than the AIT and SIT models.

Again, as with the case in figure 1(*a*), the effects of surrounding bubbles and the walls of the experimental container are deemed negligible in their effect on the experimental results as their distances are significantly greater than the thermal boundary layer thickness $\delta_T$, which we can approximate as $\delta_T = \sqrt{\alpha t} \approx R/2Ja$ (Dergarabedian 1953). This allows us to attribute the decreased growth rate in the early stages of growth to the limiting inertia, rather than limited thermal diffusion due to the disruption of the boundary layer (Enríquez *et al.* 2014).

Numerical modelling of the growth of sodium bubbles was performed by Dalle Donne & Ferranti (1975) who coupled the energy and RP equations directly, and solved them with a Runge–Kutta solver. Prosperetti & Plesset (1978) additionally included the thin thermal boundary layer assumption of Plesset & Zwick (1954) to simplify the energy equation. These bubbles are initiated at close to their critical size, and capillary effects therefore play a significant role in the dynamics of the bubbles.

Figure 2 tracks the bubble radius $R$ for cases representing (*a*) high, (*b*) moderate and (*c*) low superheats, respectively, compared with the MRG and IT model predictions. We can see from these plots that the AIT and SIT models, with capillary effects included, provide better agreement with the numerical data across the range of superheats. During the early stages of the bubble growth, the MRG model fails to capture the acceleration of the initially static bubble. This leads to the overprediction of the velocity and, subsequently, the radius of the bubble as seen for each of the three cases in figure 2(*a–c*). This overprediction does not occur for the AIT and SIT models, which capture these dynamic inertial effects. Little disagreement between the FIT and MRG models is seen due to the strong effects of capillarity in these near critically sized bubbles, which is not included in either model. During the late stages of the bubble growth, the agreement between all our IT models and the MRG model improves, as with previous cases. When the bubble has grown to the point where the dynamic inertial effects have stabilised, the growth is determined entirely by thermal effects. In the case of the low superheat, shown in figure 2(*c*), some disagreement

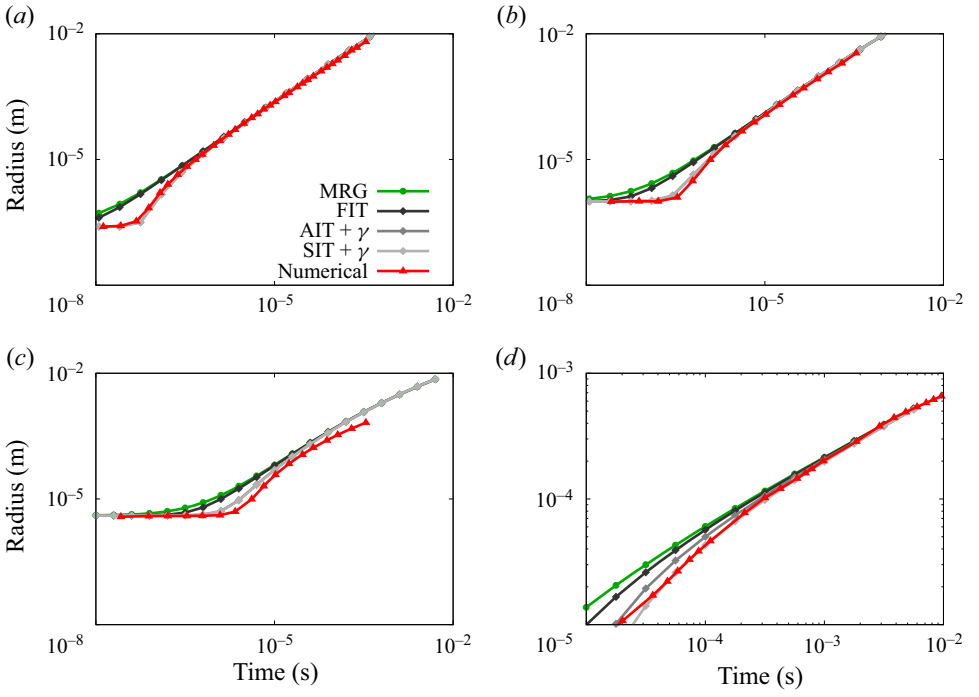


Figure 2. A comparison of the predictions of the MRG and IT models with the numerical studies of (*a*) high, (*b*) moderate and (*c*) low superheats from the work of Prosperetti & Plesset (1978), and (*d*) Robinson & Judd (2004).

between the results of Prosperetti & Plesset (1978) and the MRG model, and by extension the SIT model, is observed at larger time scales. This is attributed to the invalidity of the thin thermal boundary layer approximation at low $Ja$ where additional terms ignored in the PZ model become important (Plesset & Zwick 1954; Avdeev 2016).

Robinson & Judd (2004) perform similar numerical calculations, investigating the transition from surface tension- to thermally controlled growth of water vapour bubbles across a range of operating conditions. Their analysis shows that the assumptions in the MRG model are invalid at low $Ja$, showing disagreement with their results for $Ja < 10$. This is attributed to the theoretical limits of the PZ model, which is not accurate for $Ja < 4$ (Avdeev 2016). We account for this disparity by considering the changing inertial driving force in our IT models. Figure 2(*d*) shows vastly improved agreement between the results of Robinson & Judd (2004) and the AIT and SIT models when compared with the MRG model for $Ja = 9$. When the IT models are compared with each other, there is slightly better agreement visible with the SIT model than the AIT model, which will be elaborated on in the next section. Note that the bubble radius data from Robinson & Judd (2004) are offset by the initial radius, and the time data are offset by a thermal time constant, which is the time taken for the system to react to a change in the thermal environment and is given as $t_c = 4\gamma^2/(9\alpha\Delta P^2)$.

### 3.3. *The effect of viscosity*

So far, we have only analysed bubble growth in the absence of viscous effects. Viscosity has been shown to be largely insignificant in many of the cases analysed in literature

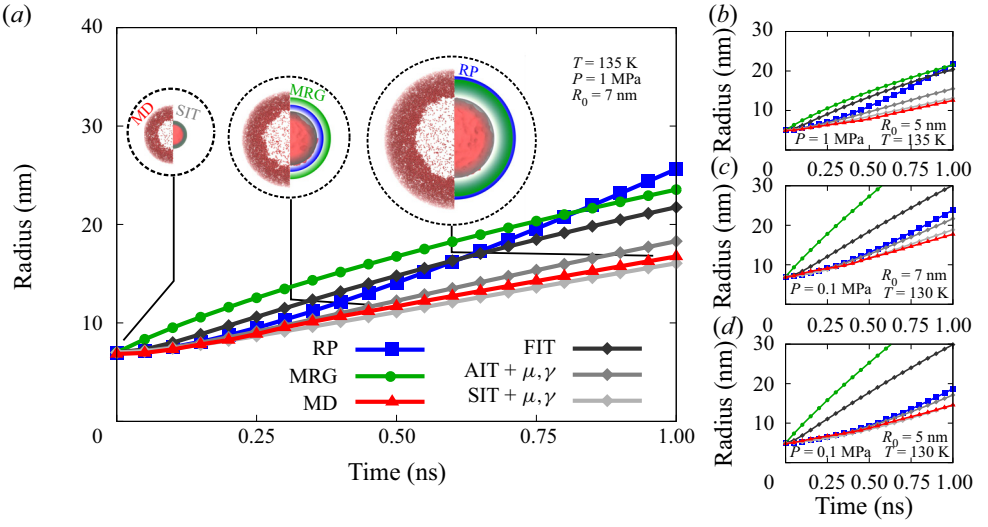


Figure 3. Comparison of the predictions of the RP, MRG and IT models with the MD simulations for four different conditions; (*a*) $R_0 = 7$ nm, $T = 135$ K and $P = 1$ MPa; (*b*) $R_0 = 5$ nm, $T = 135$ K and $P = 1$ MPa; (*c*) $R_0 = 7$ nm, $T = 130$ K and $P = 0.1$ MPa; and (*d*) $R_0 = 5$ nm, $T = 130$ K and $P = 0.1$ MPa. Inset in (*a*) is a series of simulation snapshot segments (left) alongside the measured bubble profile and model predictions at times of 0, 0.5 and 1 ns. Note the symbols $\gamma$ and $\mu$ represent the inclusion of surface tension and viscosity, respectively, in the calculation of the AIT and SIT models.

(Robinson & Judd 2004), and so is typically not included in numerical investigations (Dalle Donne & Ferranti 1975; Lee & Merte 1996). However, for critically sized bubbles at near-spinodal conditions, viscosity becomes one of the determining factors in the growth rate of the bubble (Avdeev 2016, p. 63). These conditions are difficult to produce experimentally. The small critical radii near the spinodal mean that it is very likely that a nucleation event will occur in an unplanned location, making it harder to study. Combined with the difficulties of measurement on the length and time scales necessary to capture the bubble growth in sufficient detail, this means that experimental data are not readily available to make comparisons. Thus, to validate our model predictions for bubble growth within this regime, we performed molecular dynamics (MD) simulations (details in the supplementary material).

Our MD simulations allow us to measure the growth of argon vapour bubbles with high spatial and temporal resolution. Simulations were performed with bubbles of initial radius 5 nm and 7 nm, each at two operating conditions; temperatures of 130 K and 135 K, and pressures of 0.1 MPa and 1 MPa, respectively. These cases have Reynolds numbers in the range $Re = 2.6$–$4.7$, meaning that viscous effects are of greater importance here than previous cases. The value of $\tau_{RP}/\tau_{MRG}$ ranges from 0.01–0.4, permitting the SIT model to be used for these cases. The plots in figure 3 compare the MD results with the predictions of the RP, MRG and IT models. Inset in figure 3(*a*) is a series of simulation snapshots showing a section of the MD simulation alongside the measured bubble profile and the model predictions. We consistently see that the MRG model overpredicts the initial growth rate. The RP prediction matches the early stage growth rate, but overpredicts at later stages. We can see excellent agreement with the SIT model predictions for the entire timespan for each of the cases, along with reasonable agreement of the AIT model.

These results imply consistently improved agreement of the SIT model over the AIT model, despite the additional simplifications made in the derivation of the SIT model.

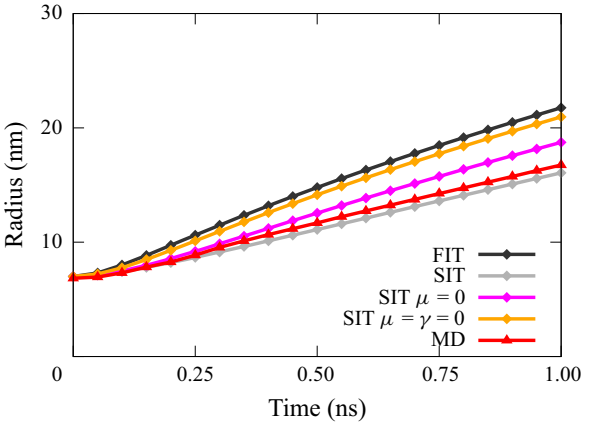


Figure 4. Comparison of the predictions of the SIT model with and without viscosity and capillarity with the MD simulations.

From the derivation, we would expect the SIT model to underpredict the radius of the bubble as it predicts a greater cooling of the bubble than the available inertia would allow as the bubble accelerates from rest. However, the linear temperature–pressure relationship used in the derivation of the MRG model, and through it the IT models (i.e. (2.7)) overpredicts the vapour pressure during the growth process (Prosperetti & Plesset 1978) and has been shown to overpredict bubble radii by up to 40 % (Lee & Merte 1996). Therefore, the apparent advantage of the SIT over the AIT only results from the cancellation of these errors, and not due to greater accuracy in modelling capacity (more details on this are given in § S5 of the supplementary material). Both the SIT and AIT models are well within this range of error for the MD cases presented in figure 3, at 15 % and 20 % respectively. Meanwhile the error in the MRG model predictions is considerably higher during the early stages of growth, only reducing to an acceptable level as the bubble grows far from its initial size.

The effect of viscosity in isolation can be studied by comparing the predictions of the SIT model with and without viscosity. Plotted in figure 4 is the case from figure 3($a$) comparing the SIT model, the SIT model without viscosity (SIT $\mu = 0$), the SIT model without viscosity and capillarity (SIT $\mu = \gamma = 0$) and the FIT model with the MD data. We can see from this plot that, in the absence of viscosity and capillarity, the SIT model is quite close to the FIT model. Figure 4 shows how viscosity can be readily included into the AIT and SIT models when needed.

## 4. Conclusions

Accounting for the changing inertial effects during the growth of an isolated vapour bubble has allowed us to extend the applicability of the existing bubble growth models. We present a new class of IT models that capture the bubble's inertially limited growth from rest, removing the singularity in the acceleration of the bubble that is present in other models. We show excellent agreement with experimental and numerical data from the literature as well as our own molecular simulations.

The FIT model describes the growth of an isolated bubble in the absence of viscous and capillary effects, and will be most applicable for describing the growth of large vapour bubbles, where the effect of viscosity and capillarity is reduced. The AIT model provides an approximate solution to the FIT model, in a manner resembling the

MRG model. Despite introducing some predictive errors, it captures the interplay between the thermal and inertial effects, with the effect of thermal diffusion becoming more relevant as the bubble grows from rest. When the time scale ratio between inertial and thermal growth is low, the SIT model can be used. This provides a simple scaling of the velocity but does not account for the interplay between the thermal and inertial effects, treating them as independently changing parameters. We have shown that in certain cases when inertial effects occur on a quicker time scale than the thermal effects, i.e. $\tau_{RP} < \tau_{MRG}$, the SIT model can give more accurate results than the AIT model despite its simpler form. This improved agreement is likely due to the cancellation of errors introduced in the model derivations (Theofanous & Patel 1976) rather than a more accurate modelling of the problem. The exact criterion for when the intrinsic error in the SIT model outweighs the systematic error in the temperature–pressure relationship remains uncertain. However, we hope that this work will motivate further research into this topic and better complete our understanding of the interplay of inertial and thermal effects. The AIT and SIT models have the added advantage that they can include effects such as viscosity and capillarity, which are needed to accurately reproduce bubble growth rates.

It is hoped that this improved understanding of homogeneous vapour bubble growth will lead to improvements in control of bubble systems. As technologies become more precise and more compact, understanding the growth behaviour of the full lifetime of vapour bubbles will become more significant. While there are additional modelling considerations that must be made to better represent these applications, such as the presence of a wall during heterogeneous bubble growth, the IT models presented here represent the most accurate theoretical approach to predict homogeneous vapour bubble growth across all length and time scales.

**Supplementary material.** Supplementary material is available at https://doi.org/10.1017/jfm.2022.734.

**Funding.** This work was supported in the UK by the Engineering and Physical Sciences Research Council (EPSRC) under Grant Nos EP/N016602/1, EP/R007438/1 and EP/V012002/1. For the purpose of open access, the authors have applied a CC BY public copyright licence to any Author Accepted Manuscript version arising from this submission. All MD simulations were run on ARCHER and ARCHER2, the UK's national supercomputing service.

**Data availability statement.** The data that support the findings of this study are openly available in the Edinburgh DataShare repository at https://doi.org/10.7488/ds/3507.

**Declaration of interests.** The authors report no conflict of interest.

**Author ORCIDs.**
Patrick Sullivan https://orcid.org/0000-0003-3547-9560;
Duncan Dockar https://orcid.org/0000-0002-5705-0581;
Matthew K. Borg https://orcid.org/0000-0002-7740-1932;
Rohit Pillai https://orcid.org/0000-0003-0539-7177.

## References

Avdeev, A.A. 2016 *Bubble Systems*. Springer.

Bardia, R. & Trujillo, M.F. 2019 Assessing the physical validity of highly-resolved simulation benchmark tests for flows undergoing phase change. *Intl J. Multiphase Flow* **112**, 52–62.

Board, S.J. & Duffey, R.B. 1971 Spherical vapour bubble growth in superheated liquids. *Chem. Engng Sci.* **26** (3), 263–274.

Brennen, C.E. 2013 *Cavitation and Bubble Dynamics*. Cambridge University Press.

Chu, K.H., Joung, Y.S., Enright, R., Buie, C.R. & Wang, E.N. 2013 Hierarchically structured surfaces for boiling critical heat flux enhancement. *Appl. Phys. Lett.* **102** (15), 151602.

DALLE DONNE, M. & FERRANTI, M.P. 1975 The growth of vapor bubbles in superheated sodium. *Intl J. Heat Mass Transfer* **18** (4), 477–493.

DERGARABEDIAN, P. 1953 The rate of growth of vapor bubbles in superheated water. *Trans. ASME J. Appl. Mech.* **20** (4), 537–545.

DERGARABEDIAN, P. 1960 Observations on bubble growths in various superheated liquids. *J. Fluid Mech.* **9** (1), 39–48.

ENRÍQUEZ, O.R., SUN, C., LOHSE, D., PROSPERETTI, A. & VAN DER MEER, D. 2014 The quasi-static growth of $CO_2$ bubbles. *J. Fluid Mech* **741**, R1.

FLORSCHUETZ, L.W., HENRY, C.L. & KHAN, A.R. 1969 Growth rates of free vapor bubbles in liquids at uniform superheats under normal and zero gravity conditions. *Intl J. Heat Mass Transfer* **12** (11), 1465–1489.

KASCHIEV, D. 2000 *Nucleation: Basic Theory with Applications*. Butterworth Heinemann.

LEE, H.S. & MERTE, H. 1996 Spherical vapor bubble growth in uniformly superheated liquids. *Intl J. Heat Mass Transfer* **39** (12), 2427–2447.

LIEN, Y. 1969 Bubble growth rates at reduced pressure. PhD thesis, Massachuesetts Institute of Technology.

MIKIC, B.B., ROHSENOW, W.M. & GRIFFITH, P. 1970 On bubble growth rates. *Intl J. Heat Mass Transfer* **13** (4), 657–666.

PLESSET, M.S. & ZWICK, S.A. 1954 The growth of vapor bubbles in superheated liquids. *J. Appl. Phys.* **25** (4), 493–500.

PROSPERETTI, A. 1982 A generalization of the Rayleigh–Plesset equation of bubble dynamics. *Phys. Fluids* **25**, 409–410.

PROSPERETTI, A. 2017 Vapor bubbles. *Annu. Rev. Fluid Mech.* **49**, 221–248.

PROSPERETTI, A. & PLESSET, M.S. 1978 Vapour-bubble growth in a superheated liquid. *J. Fluid Mech.* **85** (2), 349–368.

RAYLEIGH, LORD 1917 On the pressure developed in a liquid during the collapse of a spherical cavity. *Phil. Mag.* **34** (200), 94–98.

REINKE, P. 1997 Site deactivation techniques for suppression of nucleation in superheated liquid. *Expl Heat Transfer* **10** (2), 133–140.

ROBINSON, A.J. & JUDD, R.L. 2004 The dynamics of spherical bubble growth. *Intl J. Heat Mass Transfer* **47** (23), 5101–5113.

THEOFANOUS, T.G. & PATEL, P.D. 1976 Universal relations for bubble growth. *Intl J. Heat Mass Transfer* **19** (4), 425–429.

YASUI, K. 2018 *Acoustic Cavitation and Bubble Dynamics*. Springer.